

# Activation of SiC surfaces for vapor phase lubrication by chemical vapor deposition of Fe

D. Kim, D. Sung and A.J. Gellman\*

Department of Chemical Engineering, Carnegie Mellon University, Pittsburgh, PA 15213, USA

Received 23 December 2004; accepted 11 July 2005

Vapor phase lubrication (VPL) has been proposed as a method for lubrication of high temperature engines. During VPL, lubricants such as tricresylphosphate (TCP),  $(\text{CH}_3\text{-C}_6\text{H}_4\text{O})_3\text{P=O}$ , are delivered through the vapor phase to high temperature engine parts and react on their surfaces to deposit a thin, solid, lubricating film. Although ceramics such as SiC are desirable materials for high temperature applications, their surfaces are unreactive for the decomposition of TCP and thus not amenable to VPL. As a means of activating the SiC surface for TCP decomposition we have used chemical vapor deposition of Fe from  $\text{Fe}(\text{CO})_5$ . Modification of the SiC surface with adsorbed Fe accelerates subsequent decomposition of TCP and deposition of P and C onto the surface. In the temperature range 500–800 K, *m*-TCP decomposes more readily on Fe-coated SiC surfaces than on SiC surfaces. The C and P deposition rates depend on the thickness of the Fe film and are further enhanced by oxidation of the Fe. This work provides a proof-of-concept demonstration of the feasibility of using VPL for ceramics.

**KEY WORDS:** vapor lubrication, ceramics, SiC, tricresylphosphate

## 1. Introduction

The development of high efficiency engines operating at extremely high temperatures requires the use of lubricants that can endure temperatures over 800 K. Traditional liquid lubricants have a temperature limit of 650 K even under the most favorable conditions [1–3]. Solid lubricants can be used for high temperature applications, but are limited by the lack of a mechanism for replenishment following sliding wear. In order to overcome these difficulties, vapor phase lubrication (VPL) has been proposed as a method for the lubrication of high temperature engine components [1,2,4–6]. In this method, a vapor lubricant is continuously delivered by a carrier gas to hot engine components and reacts on their surfaces to deposit a thin, solid, lubricating film which protects the engine surfaces from sliding wear. The most widely studied vapor phase lubricants are phosphorus containing organics, including *aryl*/phosphates such as tricresylphosphate (TCP),  $(\text{CH}_3\text{-C}_6\text{H}_4\text{O})_3\text{P=O}$ . These phosphates are thought to function by decomposing on reactive metal surfaces, such as Fe and Cu, to form polyphosphate films which contain small graphitic particles [7,8]. The resulting carbon/phosphorus film provides effective lubrication [9–11].

Metals and alloys used in conventional engines have low strength and poor oxidation resistance when operated at high temperatures. In comparison, ceramic

materials such as SiC and  $\text{Si}_3\text{N}_4$  should be ideal materials for high temperature engine applications because they have many desirable high temperature properties, including high physical strength, low density, and good chemical stability [6,10,12,13]. Furthermore, the densities of ceramics are about 40% those of metals, thus reducing engine weight and improving efficiency. Lubrication of ceramics through the vapor phase or otherwise is, however, a difficult problem. Ceramics are chemically inert and as a consequence lubricants do not react readily on their surfaces [14,15]. One solution to this problem might be to activate ceramic surfaces with Fe or other metals which are known to react with vapor lubricants such as TCP [16]. If the metal were co-deposited with the lubricant from the vapor phase, then the metal activation process could be integrated into the overall scheme for VPL.

Previous research has studied the surface chemistry of trimethylphosphite,  $(\text{CH}_3\text{O})_3\text{P}$ , as a simple model for TCP, on SiC surfaces modified by Fe. That study showed that the presence of Fe on the SiC surface significantly enhanced the decomposition of trimethylphosphite [16]. In this work we have adsorbed *m*-TCP on SiC surfaces modified by deposition of Fe. *m*-TCP reacts more readily on Fe-coated SiC surfaces than on clean SiC surfaces. The surface chemistry of *m*-TCP on the Fe modified SiC surface is similar to that of *m*-TCP on the surfaces of Fe foils. On Fe foil it has been proposed that *m*-TCP decomposes via P–O bond scission to generate methylphenoxy intermediates,  $\text{CH}_3\text{-C}_6\text{H}_4\text{O-}$ , and adsorbed P atoms [17]. During heating to

\*To whom correspondence should be addressed.  
E-mail: gellman@cmu.edu

800 K, the methylphenoxy intermediates are either hydrogenated to desorb as *m*-cresol,  $\text{CH}_3\text{-C}_6\text{H}_4\text{-OH}$ , or decompose further to produce tolyl intermediates,  $\text{CH}_3\text{-C}_6\text{H}_4\text{-}$ . Some of the tolyl intermediates are hydrogenated to desorb as toluene,  $\text{CH}_3\text{-C}_6\text{H}_5$ , but the majority decompose completely resulting in  $\text{H}_2$  and CO desorption and C deposition onto the Fe surface. On the Fe modified SiC surface, the majority of the *m*-TCP decomposes through C–O bond scission to produce tolyl intermediates. Subsequently, tolyl intermediates are either hydrogenated to toluene or decompose further depositing carbon onto the surface, as they do on the Fe surface.

The work presented in this paper demonstrates the feasibility of activating SiC surfaces for *m*-TCP decomposition by using  $\text{Fe}(\text{CO})_5$  for chemical vapor deposition of Fe. During steady state exposure to the surface at high temperature, *m*-TCP is shown to decompose more readily on Fe/SiC surfaces than on clean SiC surfaces. The C and P deposition rates depend on the thickness of the Fe film and are accelerated by oxidation of the Fe. This work provides a proof-of-concept demonstration of the feasibility of using Fe CVD in conjunction with TCP for VPL of ceramics.

## 2. Experimental

All experiments were conducted in a stainless steel ultra-high vacuum (UHV) chamber with a base pressure of  $<10^{-9}$  Torr. The chamber was equipped with an ion sputter gun for surface cleaning by argon ion ( $\text{Ar}^+$ ) bombardment, a quadrupole mass spectrometer (QMS) for monitoring desorbing species during temperature programmed reaction spectroscopy (TPRS). A cylindrical mirror analyzer (CMA) was used for Auger electron spectroscopy (AES) to monitor the deposition of C and P onto the SiC surface during exposure to *m*-TCP. Standard leak valves were used to introduce high vapor pressure compounds, such as iron pentacarbonyl,  $\text{Fe}(\text{CO})_5$ , into the UHV chamber for exposure to the SiC surface. A high mass doser was used for the adsorption of *m*-TCP which has a vapor pressure of only  $10^{-9}$  Torr at room temperature [18]. This high mass doser consists of a long ( $\sim 40 \times 1.25$  cm diameter) collimating tube with a heated glass sample vial at one end. In order to expose the sample surface to low vapor pressure materials, the tube can be inserted into the vacuum chamber through a gate valve and positioned immediately in front of the sample.

The sample was an *n*-doped 6H–SiC single crystal purchased from Cree Research, Inc. and cut into a  $10 \times 10$  mm square. The SiC sample was clamped to a tantalum plate mounted by Ta wires to a liquid nitrogen reservoir on a UHV manipulator. The sample could be cooled to 150 K or heated resistively to higher than 1000 K. During heating the temperature was measured

using a K-type thermocouple spot-welded to the back of the Ta plate. The initial cleaning of the SiC sample was achieved by repeated cycles of  $\text{Ar}^+$  ion bombardment followed by annealing to 1000 K. Routine sample preparation was accomplished by 1.0 keV  $\text{Ar}^+$  ion sputtering for 50 min at 200 K followed by annealing at 850 K for 5 min. The  $\text{Ar}^+$  ion sputtering and annealing process does not produce a stoichiometric, single crystalline SiC surface. It leaves the surface with many defects and an excess of carbon because the Si preferentially evaporates during annealing [19–22]. The cleaning treatment does, however, remove the C, P, and Fe deposited during the course of experiments and does create a highly reproducible surface. Since the objective of this study is to model a process that occurs under highly non-ideal conditions it was not deemed necessary that the initial surface be perfectly clean or single crystalline.

Activation of the SiC surface with Fe was performed by exposing it to  $\text{Fe}(\text{CO})_5$  vapor at a pressure of  $2 \times 10^{-8}$  Torr and a sample temperature of 600 K. Exposure for 12 min under these conditions was sufficient to deposit an Fe film on the SiC surface with an Fe:Si elemental ratio of about 1.7:1 as determined by AES and using elemental sensitivities of 0.21 for Fe and 0.35 for Si. For some experiments the Fe modified SiC surface was intentionally oxidized by exposing it to oxygen at a pressure of  $2 \times 10^{-8}$  Torr for 5 min with the SiC surface held at 800 K.

To perform TPRS experiments, the sample was first sputtered, annealed and then cooled to 160 K. *m*-TCP was heated to 343 K (70 °C) in the glass vial of the high mass doser to increase its vapor pressure and generate a useful flux from the end of the collimating tube. The tube was moved into the chamber to position its end approximately 5 mm from the sample surface. Under these conditions, the *m*-TCP vapor can be adsorbed onto the sample surface without undue contamination of the UHV chamber. After adsorption of the *m*-TCP, the sample was positioned in front of the QMS and heated at a constant rate of 2 K/s. During heating, the QMS monitored the signals at five mass-to-charge ratios ( $m/q$ ) simultaneously as a function of temperature.

In order to determine the effects of surface activation by Fe on the rate of TCP decomposition and C and P deposition, the clean and Fe-activated SiC surfaces were exposed to continuous fluxes of *m*-TCP at temperatures of 500, 650, and 800 K. During the course of the exposure to *m*-TCP, the composition of the surface was monitored using AES. The uptake curves of C and P were measured on the clean SiC surface, on surfaces modified by different coverages of Fe and on surfaces modified by different coverages of oxidized Fe.

*m*-TCP,  $(\text{CH}_3\text{C}_6\text{H}_4\text{O})_3\text{P=O}$ , at 97% purity was purchased from Acros Organics. Before use, one fifth of the sample volume was evaporated from the sample vial for purification. Iron pentacarbonyl,  $\text{Fe}(\text{CO})_5$ , at 99%

purity was obtained from Aldrich Chemical Company and was purified by freeze–pump–thaw cycles using a gas manifold before introduction into the UHV chamber. The purity of all chemicals was verified by their mass spectra. The  $\text{Fe}(\text{CO})_5$  sample vial was kept in a Dewar flask containing ice water when not in use.  $\text{Fe}(\text{CO})_5$  is known to undergo thermal decomposition to deposit Fe on metal and ceramic surfaces at temperatures above 500 K [23–25].

### 3. Results and discussion

#### 3.1. Fe/SiC and O/Fe/SiC surfaces

The compositions of the clean and Fe-activated SiC surfaces have been determined using AES. Figure 1 shows the Auger spectra of the clean SiC surface, the Fe/SiC surface and the oxidized Fe/SiC surface. The Auger spectrum of the clean SiC surface reveals the Si peak at 88 eV and the C peak at 270 eV. The additional peaks at 213 and 510 eV reveal the presence of embedded Ar due

to sputtering and residual O, respectively. The C:Si elemental ratio of the clean surface is roughly 1.2 as determined using the Auger elemental sensitivities (0.35 for Si and 0.19 for C) at a primary beam voltage of 3 keV [26]. This ratio indicates that the surface is slightly enriched in carbon. Although this is not a stoichiometric SiC surface, the cleaning process was chosen to give a reproducible starting point for further study of the surface chemistry. The Fe/SiC surface was produced by exposure of the SiC surface to  $\text{Fe}(\text{CO})_5$  at  $2 \times 10^{-8}$  Torr for 12 min while annealing the SiC surface at 600 K. The surface exhibits Fe peaks at 44, 596, 650 and 704 eV. The Fe film thickness was determined to be  $d_{\text{Fe}} = 2.6 \text{ \AA}$  using the attenuation of the Si signal, as described below. In addition, the decomposition of the  $\text{Fe}(\text{CO})_5$  leads to a slight increase in the C concentration relative to Si and some O deposition. The Fe/SiC surface was oxidized by heating to 800 K and exposure to  $\text{O}_2$  at a pressure of  $2 \times 10^{-8}$  Torr for 5 min. Oxidation of the Fe/SiC surface results in an increase in the intensity of the oxygen peak at 510 eV. In addition, there is an obvious change in

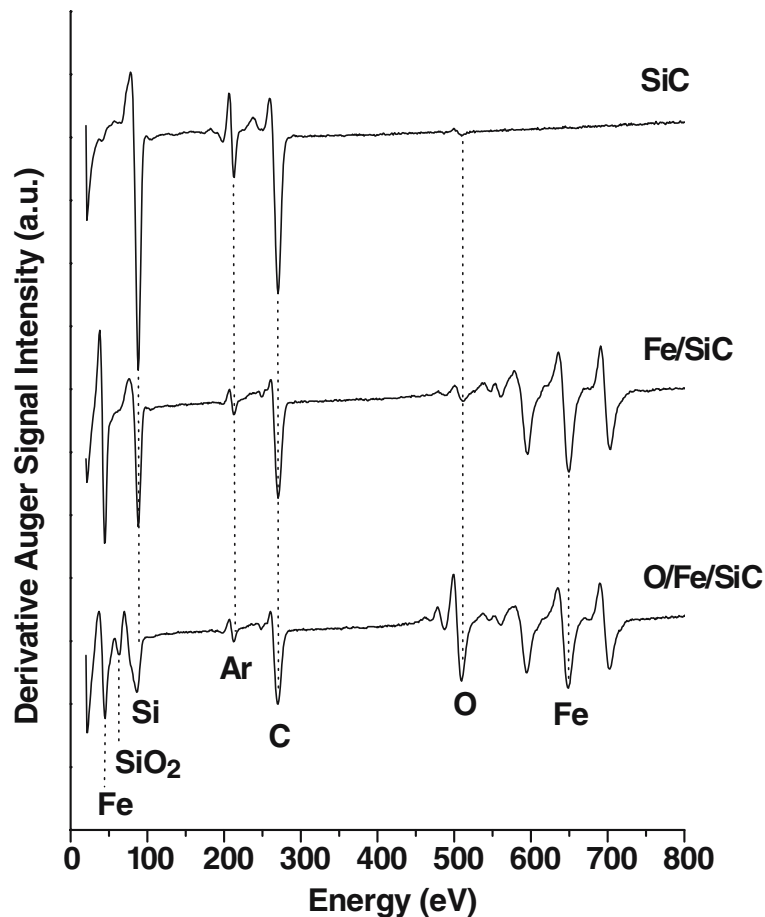


Figure 1. Auger spectra of SiC, Fe/SiC and O/Fe/SiC surfaces. The clean SiC surface was obtained by the 1.0 kV  $\text{Ar}^+$  ion sputtering for 50 min at 200 K followed by annealing at 850 K for 5 min. The Fe/SiC surface was produced by exposure of the SiC surface to  $\text{Fe}(\text{CO})_5$  at  $2 \times 10^{-8}$  Torr for 12 min with the surface at 600 K. The Fe film thickness was determined to be  $d_{\text{Fe}} = 2.6 \text{ \AA}$ . Subsequent oxidation of the surface was performed by exposure to  $\text{O}_2$  at a pressure  $2 \times 10^{-8}$  Torr for 5 min with the surface at 800 K.

the shape of the Si peak and the appearance of a small peak at 63 eV. Sneh *et al.* reported AES spectra during SiO<sub>2</sub> growth on Si(100), which showed the 63 eV peak of stoichiometric SiO<sub>2</sub> and the O (KLL) feature at 509 eV [27]. The appearance of the 63 eV peak after oxidation of the Fe/SiC surface indicates that some of the surface Si was oxidized. In addition, we expect that the Fe was oxidized although that is difficult to demonstrate on the basis of Auger spectra.

The Fe film thickness,  $d_{\text{Fe}}$ , was estimated using the attenuation of the intensity of the Si Auger signal,  $I_{\text{Si}}$ , from the SiC substrate and the following equation [28].

$$I_{\text{Si}} = I_{\text{Si}}^0 \cdot \exp\left(\frac{-d_{\text{Fe}}}{\lambda_{\text{Fe}}(E_{\text{Si}}) \cdot \cos\theta}\right) \quad (1)$$

The terms in this expression are as follows:  $I_{\text{Si}}^0$  is the Si Auger intensity of clean SiC substrate,  $d_{\text{Fe}}$  is the thickness of the Fe film,  $\lambda_{\text{Fe}}(E_{\text{Si}})$  is the mean free path through Fe of Si Auger electrons with a kinetic energy of  $E_{\text{Si}}=88$  eV, and  $\theta$  is the angle between the surface normal and the direction of electron detection. The detection angle of our CMA (PHI model 15–155) is  $\theta=42^\circ$ . Reported measurements of electron mean free paths indicate that Si electrons with a kinetic energy of  $E_{\text{Si}}=88$  eV have a mean free path through Fe of  $\lambda_{\text{Fe}}(E_{\text{Si}})=5.0 \text{ \AA}$  [29,30]. Equation (1) then yields  $d_{\text{Fe}} = 3.7 \ln(I_{\text{Si}}^0/I_{\text{Si}})$ . The underlying assumption in using this expression to determine the Fe film thickness from the Auger spectra is that the Fe is distributed evenly across the surface rather than growing in the form of clusters. If Fe grows in the form of clusters then equation (1) will only provide a rough estimate of the average Fe film thickness. Although Fe film growth has not been studied on SiC surfaces it has been studied on Si. Fe films grown to thicknesses of a few monolayers on clean Si(100) substrates exhibit island growth at low coverages followed by coalescence into a continuous film at high coverages [31–35]. In the study of the initial stages of Fe CVD onto Si(100), its morphology is characterized by formation of small clusters. Because the activation barrier for thermal decomposition of the Fe precursor on Fe is lower than that for decomposition on Si, deposition of the Fe on existing Fe clusters proceeds faster than nucleation on Si. Thus, three-dimensional Fe growth is kinetically favored over layer-by-layer growth in the initial stages of Fe CVD onto Si(100). However, the nucleation rate increases with increasing substrate temperature in the range 388–483 K, giving a higher density of stable nuclei, resulting in smaller island sizes and a smoother steady-state surface morphology. Previous STM and X-ray reflectivity measurements have shown that the average cluster density increases with increasing substrate temperature [31,33]. The deposition temperature of 600 K used in this work may result in small dense clusters distributed across the surface.

The decomposition of *m*-TCP has been studied on Fe/SiC surfaces oxidized by low pressure exposure to O<sub>2</sub> gas with the surface held at 600 K. The stoichiometric oxides of Fe that might be produced include Fe<sub>3</sub>O<sub>4</sub>, Fe<sub>2</sub>O<sub>3</sub> and FeO. In order to understand which oxidation state of Fe was produced by this treatment, we have reviewed previous work on the oxidation of Fe under UHV conditions. Previous studies have suggested that FeO formation is favored at low O<sub>2</sub> exposures ( $\sim 10 \text{ L}$ ) with surface temperatures of  $<800 \text{ K}$  [36–38]. In our work, the O<sub>2</sub> exposure to the Fe/SiC surface was  $\sim 6 \text{ L}$  at 800 K, suggesting that the oxidation state of the Fe on our SiC surface is predominantly FeO. This suggestion is supported by the O/Fe AES peak ratio. Langell *et al.* reported an O/Fe AES peak ratio of 4.1 for an Fe<sub>2</sub>O<sub>3</sub>-like surface composition and a ratio of 3.7 for an Fe<sub>3</sub>O<sub>4</sub>-like surface composition [39]. The O/Fe AES peak ratio observed in our studies was 1.1 for the O/Fe/SiC surfaces, which would be consistent with the formation of FeO. Understanding the oxidation state of the Fe on our surface is complicated by the fact that the Auger spectra indicate that some of the oxygen is present in the form of SiO<sub>2</sub>. This would reduce the O/Fe ratio in the iron oxide and thus strengthens the suggestion that the oxidation state of the Fe is FeO.

### 3.2. TPRS of *m*-TCP on SiC and Fe/SiC surfaces

Temperature programmed reaction spectroscopy has been used to probe the mechanism of *m*-TCP decomposition on the clean SiC surface and the Fe/SiC surface. This work has been aimed primarily at identifying the species produced by *m*-TCP decomposition and the temperature ranges in which they desorb from the surface. Figure 2 illustrates the TPR spectra of one monolayer of *m*-TCP on the clean SiC surface. Desorption spectra obtained following increasing exposures to *m*-TCP have revealed that an exposure of  $\sim 2$  min using the high molecular weight doser is sufficient to deposit one monolayer of *m*-TCP on the surface. Higher exposures lead to desorption of *m*-TCP multilayers during heating. The TPR spectra were generated by monitoring the signals at  $m/q=2$  (H<sub>2</sub><sup>+</sup>), 28 (CO<sup>+</sup>), 91 (CH<sub>3</sub>C<sub>6</sub>H<sub>4</sub><sup>+</sup>), 92 (CH<sub>3</sub>C<sub>6</sub>H<sub>5</sub><sup>+</sup>) and 107 (CH<sub>3</sub>C<sub>6</sub>H<sub>4</sub>O<sup>+</sup>) during heating at 2 K/s. *m*-TCP itself has ionization fragments at  $m/q=91$  (CH<sub>3</sub>C<sub>6</sub>H<sub>4</sub><sup>+</sup>), 92 (CH<sub>3</sub>C<sub>6</sub>H<sub>5</sub><sup>+</sup>) and 107 (CH<sub>3</sub>C<sub>6</sub>H<sub>4</sub>O<sup>+</sup>). The desorption features at 260 K indicate molecular desorption of *m*-TCP. The broad desorption peaks at 645 K for fragments with  $m/q=91$  and 92 reveal toluene desorption. The TPR spectra of H<sub>2</sub> and CO increase above 500 K. Allendorf *et al.* studied the adsorption and desorption of hydrogen atoms on a polycrystalline SiC surface [40]. They observed that hydrogen recombines and desorbs as H<sub>2</sub> on the polycrystalline SiC surface producing peaks at 975 and 1130 K. They suggested

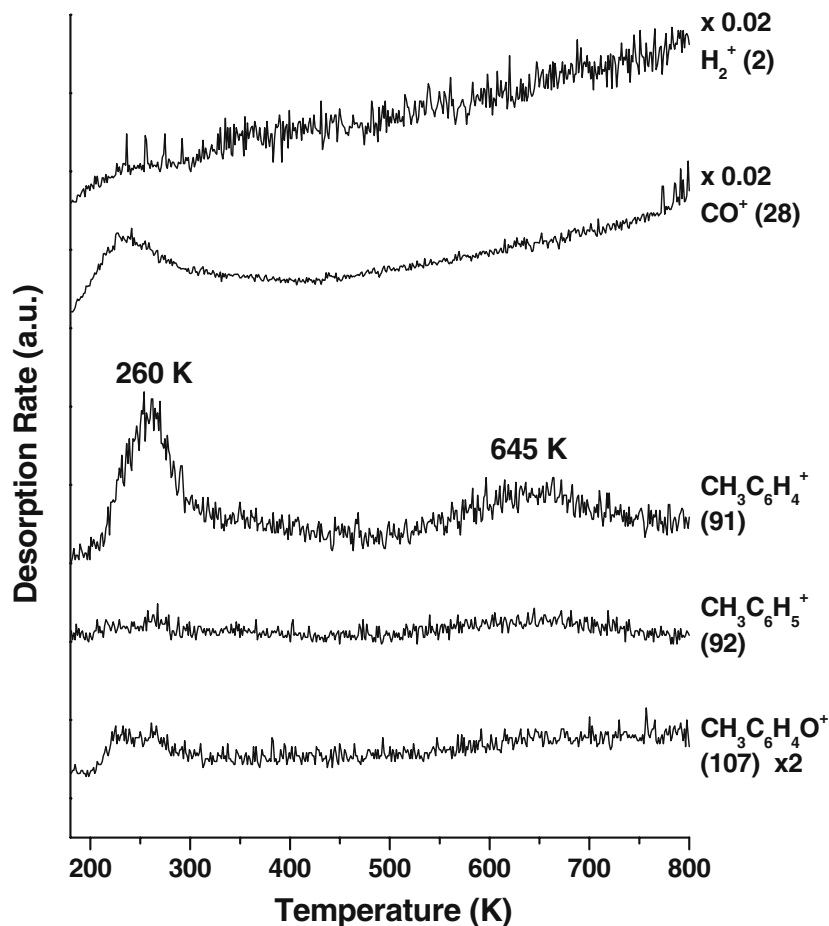


Figure 2. TPR spectra of *m*-TCP on the SiC surface for ionization fragments with  $m/q=2$  ( $\text{H}_2^+$ ), 28 ( $\text{CO}^+$ ), 91 ( $\text{CH}_3\text{C}_6\text{H}_4^+$ ), 92 ( $\text{CH}_3\text{C}_6\text{H}_5^+$ ) and 107 ( $\text{CH}_3\text{C}_6\text{H}_4\text{O}^+$ ). The *m*-TCP coverage was  $\sim 1$  ML. The sample heating rate was 2 K/s. On the SiC surface, some *m*-TCP desorbs molecularly at 260 K, while the remainder decomposes through C–O bond cleavage to produce tolyl intermediates,  $\text{CH}_3\text{C}_6\text{H}_4^+$ , which are hydrogenated to desorb as toluene at  $T=645$  K.

that the unusually broad width of the desorption peaks is due to a distribution of surface binding energies for H atoms. In our spectra, the TPR spectra of  $\text{H}_2$  and CO continue to increase in intensity up to  $T=1000$  K without the appearance of resolvable peaks. It is not certain whether this desorption comes from the SiC surface or from the sample holder as it heats up. The conclusion to be drawn from the TPR spectra is that on the SiC surface, some *m*-TCP desorbs molecularly while the remainder decomposes through C–O bond scission to form tolyl groups which can be hydrogenated to toluene at  $T=645$  K.

Fe has been deposited on the SiC surface in order to activate the surface towards decomposition of vapor phase lubricants such as *m*-TCP. The TPR spectra of *m*-TCP on the Fe/SiC surface shown in figure 3 are clearly different from the TPR spectra of *m*-TCP on the clean SiC surface. While the SiC substrate is unreactive, the deposition of an Fe film has activated the surface for *m*-TCP decomposition. Toluene evolves into the gas phase over a temperature range of 300–500 K, while CO desorbs over the temperature range 300–450 K. There is

a small  $\text{H}_2$  desorption peak observed at 560 K. The temperature range over which toluene, and  $\text{H}_2$  desorb is similar to that observed on the clean Fe surface in previous work [17]. On the clean Fe surface, decomposition of *m*-TCP was observed to lead to desorption of toluene in peaks at 355 and 500 K, desorption of  $\text{H}_2$  at 550 K, and desorption of CO at 700 K. Thus the Fe/SiC surface has some similarities to the bare Fe surface and the deposition of Fe has clearly activated the SiC surface for *m*-TCP decomposition. The primary difference between the Fe and Fe/SiC surfaces is the desorption of CO which appears to occur at higher temperature on the clean Fe surface than on the Fe/SiC surface. It is possible that the C in the SiC is oxidized by the oxygen liberated by the decomposition of the *m*-TCP and that this can occur at lower temperatures than the oxidation of C on the Fe surface. On the Fe/SiC surface the majority of the *m*-TCP decomposes through C–O bond cleavage to form tolyl intermediates which can be hydrogenated to toluene at  $T=300$ –500 K. Subsequently, tolyl groups decompose further to  $\text{C}_x\text{H}_y$  fragments, which desorb as  $\text{H}_2$  and CO at 600–800 K. The

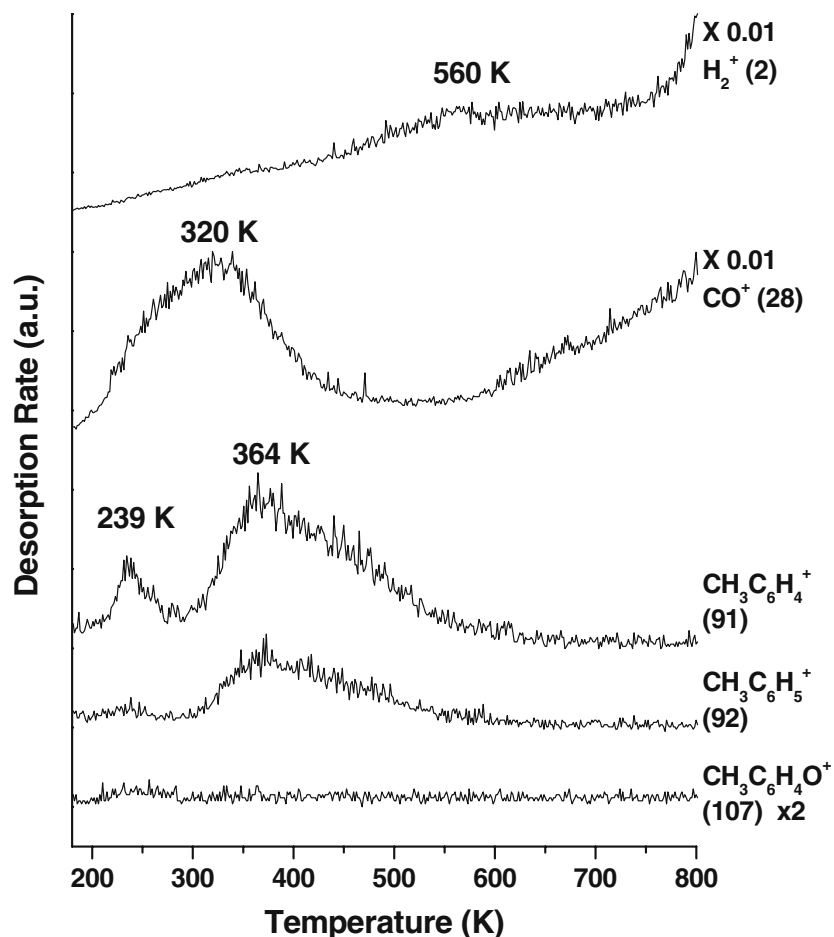


Figure 3. TPR spectra of *m*-TCP on the Fe/SiC surface for ionization fragments with  $m/q=2$  ( $\text{H}_2^+$ ), 28 ( $\text{CO}^+$ ), 91 ( $\text{CH}_3\text{C}_6\text{H}_4^+$ ), 92 ( $\text{CH}_3\text{C}_6\text{H}_5^+$ ) and 107 ( $\text{CH}_3\text{C}_6\text{H}_4\text{O}^+$ ). Prior to *m*-TCP adsorption the surface was modified by deposition of an Fe film with an Fe/Si elemental ratio of about 1.7:1 as determined by AES. The sample heating rate was 2 K/s. On the Fe/SiC surface, a little *m*-TCP undergoes molecular desorption, while the majority decomposes through C–O bond scission to form tolyl intermediates,  $\text{CH}_3\text{C}_6\text{H}_4^+$ , which are hydrogenated to desorb as toluene at  $T=300\text{--}500$  K.

primary point is that the kinetics of *m*-TCP decomposition on the Fe/SiC surface are different from those on the SiC surface and that decomposition appears to occur at lower temperatures.

Auger spectroscopy has been used to monitor the composition of the surface during Fe deposition and following *m*-TCP decomposition. Figure 4 shows the Auger spectra of the clean SiC surface, the Fe/SiC surface and both surfaces after TPRS of *m*-TCP. Initially, the C:Si elemental ratio is 1.2 on the SiC surface, as determined from the Auger elemental sensitivities (0.35 for Si, 0.19 for C, and 0.53 for P at a primary beam voltage of 3 keV) [26]. After the TPRS of *m*-TCP on the SiC surface, the C:Si and P:Si elemental ratios are 2.1 and 0.03, revealing an increase of 80% in the surface carbon composition. The signal due to P is negligible on the clean SiC surface but can be observed in the AES spectrum of the surface after decomposition of *m*-TCP. Thus the Auger spectra reveal that there has been some decomposition of *m*-TCP on the SiC surface. After the TPRS of *m*-TCP on the Fe/SiC surface, the C:Si and

P:Si elemental ratios are 3.8 and 0.04, respectively, indicating a greater degree of decomposition on the Fe/SiC surface than on the clean SiC surface. Both TPRS and AES results indicate that there is more decomposition of *m*-TCP on the Fe/SiC surface than on the clean SiC surface, leading to greater C and P deposition.

### 3.3. C/P film deposition rates during *m*-TCP exposure

In order to demonstrate the potential for use of Fe modification as a means of activating the SiC surface for VPL, we have studied the uptake of C and P onto the surface during exposure to *m*-TCP. By comparing the uptake rates on the clean SiC and the Fe/SiC surfaces we are able to observe the effects of Fe activation directly. In addition, we have examined the effects of Fe oxidation on its ability to activate the decomposition of *m*-TCP. Under conditions of VPL, surfaces are exposed continuously to compounds such as *m*-TCP that decompose to deposit lubricous films. We have

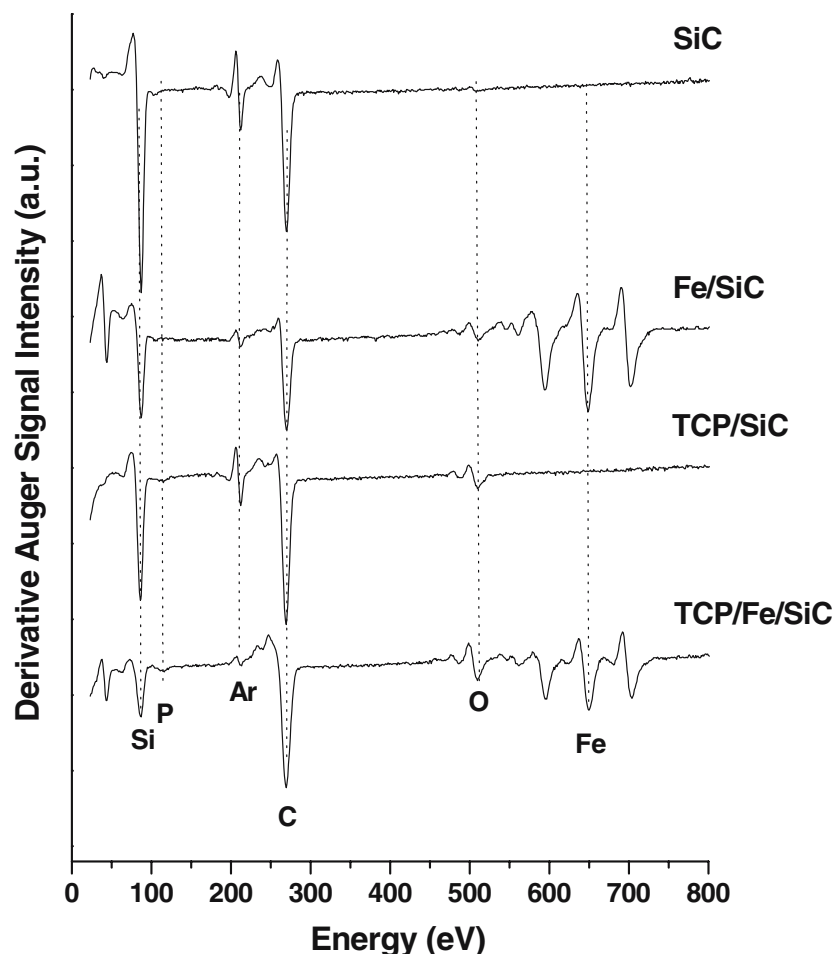


Figure 4. Auger spectra of the clean SiC surface, the Fe/SiC surface, and both surfaces after TPRS of *m*-TCP. The Fe/SiC surface was activated by the exposure of the SiC surface to  $\text{Fe}(\text{CO})_5$  at  $2 \times 10^{-8}$  Torr for 12 min with the surface at 600 K. The Fe film thickness was determined to be  $d_{\text{Fe}} = 3.0$  Å. TPRS spectra were obtained with *m*-TCP coverages of  $\sim 1$  ML. The increases in the C and P concentrations following *m*-TCP decomposition are greater on the Fe/SiC surface than on the SiC surface.

attempted to mimic this process by exposing the SiC, Fe/SiC, and O/Fe/SiC surfaces to *m*-TCP at elevated temperatures while using Auger spectroscopy to monitor the deposition of C and P onto the surfaces. Figure 5 illustrates the Auger spectra of the O/Fe/SiC surface after TCP exposure times in the range 0–15 min with the surface at 500 K. For reference, exposures of  $\sim 2$  min are needed to adsorb 1 ML of *m*-TCP with the surface at low temperature. The Auger spectra of the surface after *m*-TCP exposure clearly reveal the presence of P and an increase in the coverage of C, indicating thermal decomposition of *m*-TCP. The C and P Auger peaks increase in intensity, while those of Si and Fe decrease with increasing *m*-TCP exposure. The shape of the C peak observed following decomposition of *m*-TCP on the O/Fe/SiC surface suggests the formation of a layer of graphitic carbon on the surface [41,42]. Clearly, the SiC surface modified by the presence of oxidized Fe has been activated for *m*-TCP decomposition.

In order to study the evolution of the surface composition during exposure to *m*-TCP, the Auger signals have been monitored as a function of time during *m*-

TCP exposure to several different surfaces at temperatures in the range  $T = 500$ – $800$  K. Figure 6 shows the evolution of the Si, P, C, O and Fe concentrations as a function of time during exposure of the O/Fe/SiC surface at  $T = 500$  K. The concentration of each element is estimated from the Auger peak-to-peak intensities scaled by their Auger elemental sensitivities (0.35 for Si, 0.53 for P, 0.19 for C, 0.51 for O and 0.21 for Fe at a primary beam energy of 3 keV). In this case it is the Fe peak at 650 eV that has been monitored as a function of time. The C and P coverages increase, while the O, Fe, and Si coverages decrease with increasing *m*-TCP exposure. The decrease in the apparent coverages of Fe and Si are attributed to screening of their Auger signals as C and P are deposited onto the SiC surface.

As mentioned earlier, it has been suggested that a carbon containing polyphosphate film generated by TCP decomposition is necessary for effective VPL [7,9,10]. The hypothesis motivating this work has been that an Fe film on the SiC surface can accelerate the formation of such a lubricous film. In order to verify this hypothesis, we have focused on the differences between the C/P film

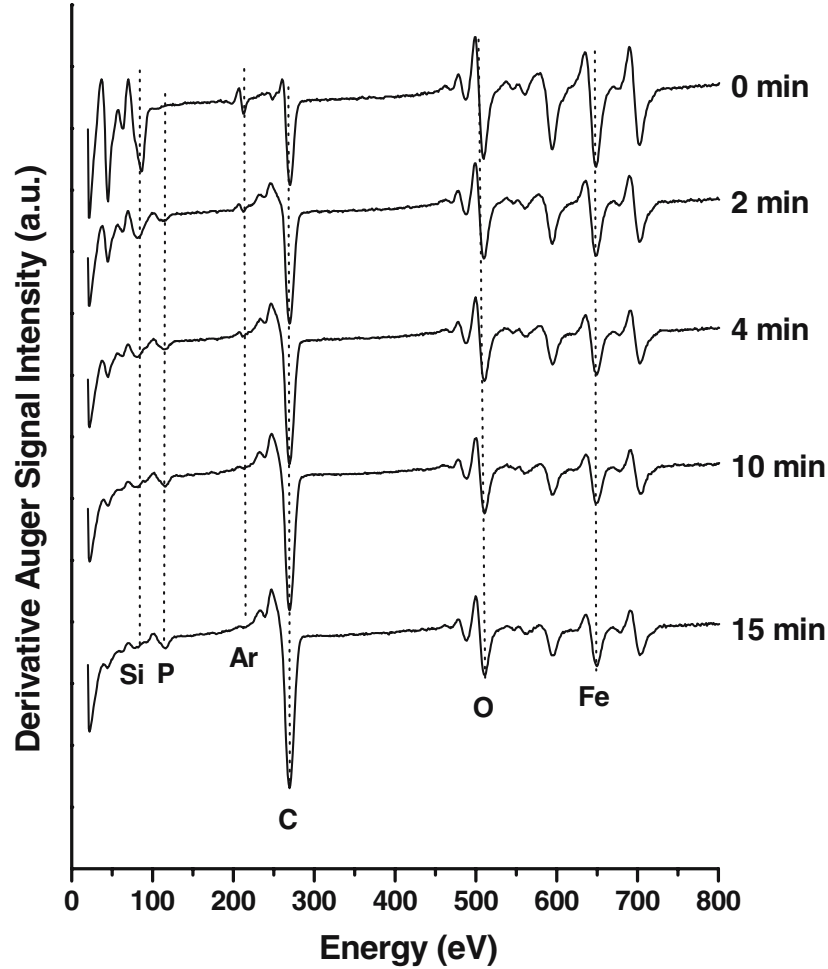


Figure 5. Auger spectra of the O/Fe/SiC surface after TCP exposures of 0, 2, 4, 10, and 15 min while heating the surface at 500 K. The exposure to *m*-TCP used conditions that deposit  $\sim 1$  ML in 2 min. The C and P Auger peaks increase, while those from Si and Fe decrease with increasing *m*-TCP exposure.

thicknesses on the SiC surface and the Fe/SiC surface. The experiments were performed using two different Fe film thicknesses on the SiC surfaces (one greater than 2 Å and another less than 2 Å) and exposing these to *m*-TCP at three different temperatures (500, 650, and 800 K). During exposure of the SiC surface to *m*-TCP, both C and P were deposited onto the surface and the growth of their film thicknesses were measures of the rates of *m*-TCP decomposition. Figure 7 shows the thickness of the C/P film during exposure of clean SiC, Fe/SiC, and O/Fe/SiC surfaces to *m*-TCP at 500 K. Employing the same method used in estimating the thickness of Fe films, the thickness of the C/P film,  $d_{C/P}$ , was estimated using the following equation and the attenuation of the intensity of the Si Auger signal,  $I_{Si}$ , from the SiC substrate during the deposition of the C/P film [28].

$$I_{Si} = I_{Si}^0 \cdot \exp\left(\frac{-d_{C/P}}{\lambda_{C/P}(E_{Si}) \cdot \cos\theta}\right) \quad (2)$$

The terms in the expression above are as follows:  $I_{Si}^0$  is the Si AES signal before any exposure to TCP (but with

deposited Fe),  $\lambda_{C/P}(E_{Si})$  is the mean free path of the Si Auger electrons with a kinetic energy of  $E_{Si} = 88$  eV (5.0 Å [29,30]) through the C/P film, and  $\theta$  is the angle between the surface normal and the direction of electron detection ( $\theta = 42^\circ$ ). This equation then yields  $d_{C/P} = 3.7 \ln(I_{Si}^0/I_{Si})$ . The thickness of the C/P film,  $d_{C/P}$ , does not include the attenuation due to the presence of Fe because the initial Si Auger signals,  $I_{Si}^0$ , were measured after Fe deposition but before exposure to TCP.

The C/P film thickness curves illustrated in Figure 7 clearly reveal two trends in the deposition rates. The presence of the Fe film does not have a significant effect on the TCP decomposition rate when the Fe film is  $\sim 1$  Å thick but does exhibit an effect when the Fe film thickness exceeds  $\sim 2$  Å. Then rate of deposition onto the Fe/SiC surfaces is significantly greater than on the clean SiC surface. What is more interesting is the fact that the rates of deposition onto the oxidized Fe/SiC surfaces are greater than onto the clean SiC and the Fe/SiC surfaces indicating that the activity for decomposition of *m*-TCP follows the order:

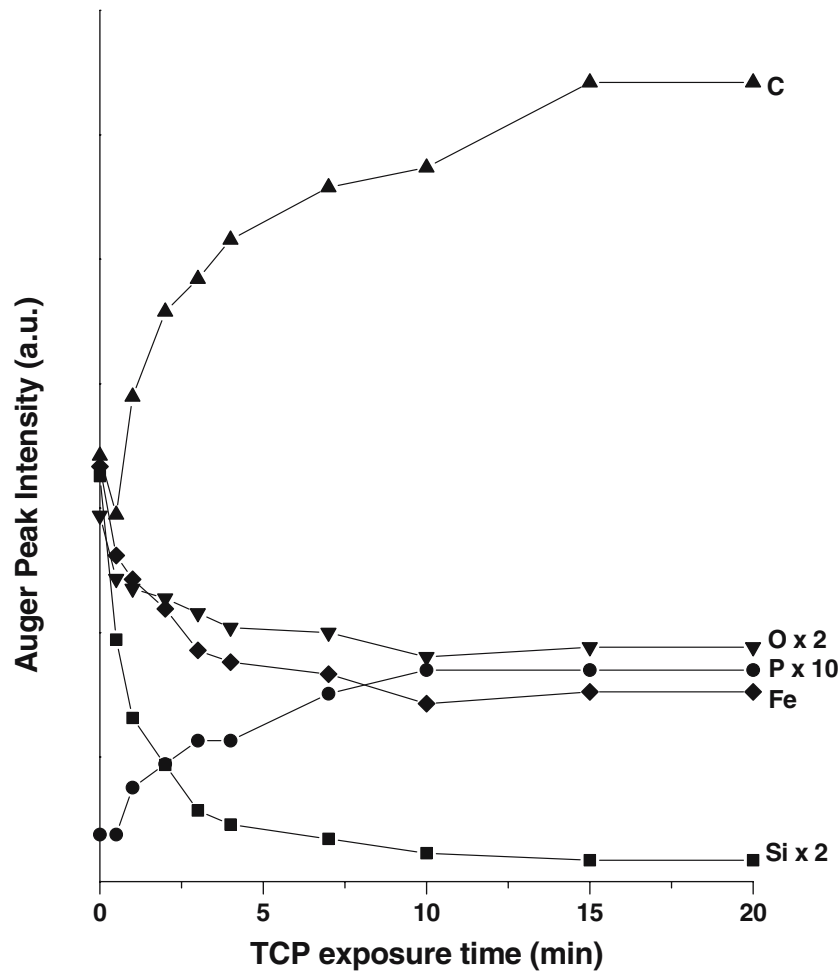


Figure 6. The relative concentrations of the Si, P, C, O, and Fe (as estimated directly from their AES signals) as a function of increasing *m*-TCP exposure while heating the O/Fe/SiC surface at 500 K. The C and P coverages increase, while O, Fe, and Si coverages decrease with increasing *m*-TCP exposure due to screening by the adsorbed film. The concentration of each element is estimated from the Auger peak-to-peak intensities scaled by their Auger elemental sensitivities (0.35 for Si, 0.53 for P, 0.19 for C, 0.51 for O and 0.21 for Fe at 3 keV primary beam voltage).

clean SiC < Fe/SiC < O/Fe/SiC

This result is consistent with those of previous studies which have shown that TCP reactivity with Fe increases with increasing oxidation state of the Fe. Those studies have shown that the reaction rates of *m*-TCP on different Fe oxides follow the order:

Fe < FeO < Fe<sub>3</sub>O<sub>4</sub> or Fe<sub>2</sub>O<sub>3</sub>

[43]. In our case, the conditions under which the Fe films were oxidized are consistent with the formation of FeO. Presumably, additional oxidation of the Fe films on our SiC surfaces would further enhance the rate of TCP decomposition. The *m*-TCP decomposition experiments illustrated in Figure 7 have also been performed at surfaces temperatures of 650 and 800 K. The uptake curves obtained at those temperatures reveal the same relative reactivities of the different surfaces.

#### 4. Conclusions

Thin Fe films can be deposited on the surface of SiC by exposure to Fe(CO)<sub>5</sub> with the surface at a temperature of ~600 K. Once activated by the deposition of Fe, the SiC surfaces will decompose vapor phase lubricants such as *m*-TCP in a manner similar to their decomposition on the Fe surface. The Fe/SiC surface is further activated by oxidation of the Fe film. These results suggest that surface activation by Fe CVD might be a viable approach to the VPL of ceramics. Fe CVD could be accomplished from the vapor phase and in conjunction with VPL by using high vapor pressure Fe containing compounds such as Fe(CO)<sub>5</sub>.

#### Acknowledgments

This work has been supported by the Air Force Office of Scientific Research under Grant No. AF49620-01-1-0069.

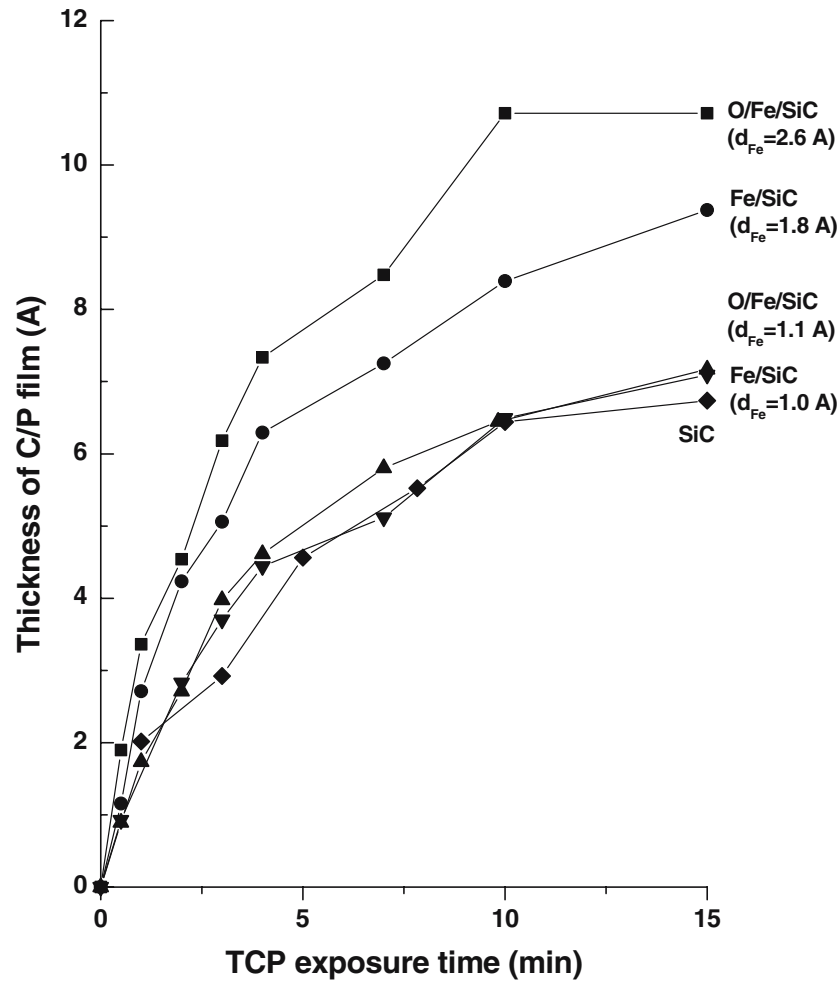


Figure 7. The increase in the C/P film thickness on the O/Fe/SiC ( $d_{Fe} = 2.6 \text{ \AA}$ ), Fe/SiC ( $d_{Fe} = 1.8 \text{ \AA}$ ), O/Fe/SiC ( $d_{Fe} = 1.1 \text{ \AA}$ ), Fe/SiC ( $d_{Fe} = 1.0 \text{ \AA}$ ) and clean SiC surfaces as a function of  $m$ -TCP exposure while heating the surfaces at 500 K. The growth rate of the C/P film thickness is indicative of the  $m$ -TCP decomposition rates on the different surfaces. The film thickness is estimated from the attenuation of the Si Auger signal after exposure to TCP.

## References

- [1] J.F. Makki and E.E. Graham, *Lubr. Eng.* 47 (1991) 199.
- [2] A.M.N. Rao, *Lubr. Eng.* 52 (1996) 856.
- [3] K.W. Van Treuren, D.N. Barlow, W.H. Heiser, M.J. Wagner and N.H. Forster, *J. Eng. Gas Turbines and Power* 120 (1998) 257.
- [4] J.F. Makki and E.E. Graham, *Trib. Trans.* 33 (1990) 595.
- [5] M. Groeneweg, N. Hakim, G.C. Barber and E.E. Klaus, *Lubr. Eng.* 47 (1991) 1035.
- [6] E.E. Graham, A. Nesarikar, N. Forster and G. Givan, *Lubr. Eng.* 49 (1993) 713.
- [7] N.H. Forster and H.K. Trivedi, *Trib. Trans.* 40 (1997) 493.
- [8] N.H. Forster, *Trib. Trans.* 42 (1999) 1.
- [9] E.E. Klaus, G.S. Jeng and J.L. Duda, *Lubr. Eng.* 45 (1989) 717.
- [10] B. Hanyaloglu and E.E. Graham, *Lubr. Eng.* 50 (1994) 814.
- [11] N.H. Forster and H.K. Trivedi, *Trib. Trans.* 40 (1997) 421.
- [12] J.L. Lauer and S.R. Dwyer, *Trib. Trans.* 34 (1991) 521.
- [13] B. Hanyaloglu, D.C. Fedor and E.E. Graham, *Lubr. Eng.* 51 (1995) 252.
- [14] E.E. Klaus, J. Phillips, S.C. Lin, N.L. Wu and J.L. Duda, *Trib. Trans.* 33 (1990) 25.
- [15] B. Hanyaloglu and E.E. Graham, *Trib. Trans.* 35 (1992) 77.
- [16] D. Ren, D. Sung and A.J. Gellman, *Trib. Lett.* 10 (2001) 179.
- [17] D. Sung and A.J. Gellman, *Trib. Int.* 35 (2002) 579.
- [18] R.M. Stephenson and S. Malanowski, *Handbook of the Thermodynamics of Organic Compounds* (Elsevier Science Publishing Co., Inc, New York, 1987).
- [19] T.L. Chu and R.B. Campbell, *J. Electrochem. Soc.* 112 (1965) 955.
- [20] V. Ramachandran, M.F. Brandy, A.R. Smith, R.M. Feenstra and D.W. Greve, *J. Appl. Phys.* 27 (1998) 308.
- [21] T. Friessnegg, M. Boudreau, P. Mascher, A. Knights, P.J. Simpson and W. Puff, *J. Appl. Phys.* 84 (1998) 786.
- [22] Q.Z. Xue, Q.K. Xue, Y. Hasegawa, I.S.T. Tsong and T. Sakurai, *Appl. Phys. Lett.* 74 (1999) 2468.
- [23] L. Sun and E.M. McCash, *Surf. Sci.* 422 (1999) 77.
- [24] M.N. Rocklein and D.P. Land, *Surf. Sci.* 436 (1999) L702.
- [25] R.B. Jackman and J.S. Foord, *Surf. Sci.* 209 (1989) 151.
- [26] L.E. Davis, N.C. MacDonald, P.W. Palmberg, G.E. Riach and R.E. Weber, *Handbook of Auger Electron Spectroscopy*, 2nd edn. (Physical Electronics Industries Inc. Minnesota, 1976).
- [27] O. Sneh, M.L. Wise, A.W. Ott, L.A. Okada and S.M. George, *Surf. Sci.* 334 (1995) 135.
- [28] G.A. Somorjai, *Chemistry in Two Dimensions: Surfaces* (Cornell University Press, Ithaca, NY, 1981).
- [29] C.J. Powell and A. Jablonski, *J. Phys. Chem. Ref. Data* 28 (1999) 19.

- [30] C.J. Powell and A. Jablonski, *Surf. Interface Anal.* 29 (2000) 108.
- [31] D.P. Adams, T.M. Mayer, E. Chason, B.K. Kellerman and B.S. Swartzentruber, *Phys. Rev. Lett.* 74 (1995) 5088.
- [32] D.P. Adams, T.M. Mayer, E. Chason, B.K. Kellerman and B.S. Swartzentruber, *Surf. Sci.* 371 (1997) 445.
- [33] B.K. Kellerman, E. Chason, D.P. Adams, T.M. Mayer and J.M. White, *Surf. Sci.* 375 (1997) 331.
- [34] J.S. Foord and R.B. Jackman, *Chem. Phys. Lett.* 112 (1984) 190.
- [35] F. Thibaudau, L. Masson, A. Cheman, J.R. Roche and F. Salvan, *J. Vac. Sci. Technol. A* 16 (1998) 2967.
- [36] B.L. Maschhoff and N.R. Armstrong, *Langmuir* 7 (1991) 693.
- [37] G.H. Vurens, M. Salmeron and G.A. Somorjai, *Surf. Sci.* 201 (1988) 129.
- [38] C. Jansson and P. Morgan, *Surf. Sci.* 233 (1990) 84.
- [39] M. Langell and G.A. Somorjai, *J. Vac. Sci. Technol.* 21 (1982) 858.
- [40] M.D. Allendorf and D.A. Outka, *Surf. Sci.* 258 (1991) 177.
- [41] D.W. Goodman, R.D. Kelley, T.E. Madey, J.T. Yates Jr. *J. Catal.* 63 (1980) 226.
- [42] J.E. Houston, D.E. Peebles and D.W. Goodman, *J. Vac. Sci. Technol. A* 1 (1983) 995.
- [43] C.S. Saba and N.H. Forster, *Trib. Lett.* 12 (2002) 135.